Jörg Gebhardt*, Guruprasad Sosale, and Subhashish Dasgupta

Non-invasive temperature measurement of turbulent flows of aqueous solutions and gases in pipes

Nichtinvasive Temperaturmessung für turbulente Rohrströmungen von wässrigen Lösungen und Gasen

https://doi.org/10.1515/teme-2020-0028
Received April 17, 2020; accepted July 14, 2020

Abstract: Accurate and responsive non-invasive temperature measurements are enablers for process monitoring and plant optimization use cases in the context of Industry 4.0. If their performance is proven for large classes of applications, such measurement principles can replace traditional invasive measurements. In this paper we describe a two-step model to estimate the process temperature from a pipe surface temperature measurement. This static case model is compared to and enhanced by computational fluid dynamic (CFD) calculations to predict transient situations. The predictions of the approach are validated by means of controlled experiments in a laboratory environment. The experimental results demonstrate the efficacy of the model, the responsiveness of the pipe surface temperature, and that state of the art industrial non-invasive sensors can achieve the performance of invasive thermowells. The non-invasive sensors are then used to demonstrate the performance of the model in industrial applications for cooling fluids and steam.

Keywords: Temperature measurement, non-invasive measurement, model-based sensing, computational fluid dynamics, boundary layer, Nußelt number, Industrie 4.0.

Zusammenfassung: Nichtinvasive Temperaturmessungen mit hoher Genauigkeit und Ansprechdynamik eröffnen neue Möglichkeiten für die Prozessüberwachung und Anlagenoptimierung im Kontext von Industrie 4.0. Wird ihre Leistungsfähigkeit für große Klassen von Anwendungen nachgewiesen, so können modellbasierte nichtinvasive Messungen traditionelle invasive Messungen ersetzen. In diesem Artikel wird ein Zwei-Stufen-Modell zur Schätzung der Prozesstemperatur angegeben, ausgehend von einer Messung der Oberflächentemperatur der Prozessleitung. Das entsprechende statische Modell wird abgeglichen mit numerischen Strömungsmechanik-Rechnungen, insbesondere zur Klärung transienter Effekte. Die modellbasierten Vorhersagen werden anhand von Experimenten im kontrollierten Laborumfeld validiert. Die Testergebnisse zeigen eine sehr gute Vorhersagekraft der Modelle sowie ein schnelles Ansprechen der Rohroberflächentemperatur. Sie belegen, dass nichtinvasive Sensoren die Leistungsfähigkeit invasiver Schutzrohrmessungen erreichen können. Die nichtinvasiven Sensoren werden schließlich benutzt, um in zwei Anwendungsfällen aus der Industriepraxis (für Kühlflüssigkeiten bzw. überhitzten Dampf) die Wirksamkeit des Modellansatzes zu demonstrieren.

Schlagwörter: Temperaturmessung, nicht-invasive Messungen, modellbasierte Sensorik, numerische Strömungsmechanik, Grenzschicht, Nußeltzahl, Industrie 4.0.

***Corresponding author: Jörg Gebhardt,** ABB Corporate Research Germany, Wallstadter Str. 59, 68526 Ladenburg, Germany, e-mail: joerg.gebhardt@de.abb.com, ORCID: https://orcid.org/0000-0001-9200-5025
Guruprasad Sosale, ABB Automation Products GmbH, Industrial Automation – Measurement & Analytics, Kallstadter Strasse 1, 68309 Mannheim, Germany
Subhashish Dasgupta, ABB Global Industries and Services Pvt. Ltd, Bangalore, India

1 Introduction – The relevance of non-invasive temperature measurement in process industries

Digitalization and Industry 4.0 have created a new industrial environment for sensors [1]. Flexible measurement solutions for monitoring and optimization that can be cost effectively and reliably installed in existing plants are key sources of new insights into industrial processes [2].

With temperature being one of the fundamental and often critical process parameters, this paper demonstrates a non-invasive approach to measuring the process temperature in a large number of common industrial processes. Such an approach can greatly simplify the engineering

Open Access. © 2020 Gebhardt et al., published by De Gruyter. This work is licensed under the Creative Commons Attribution 4.0 International License.

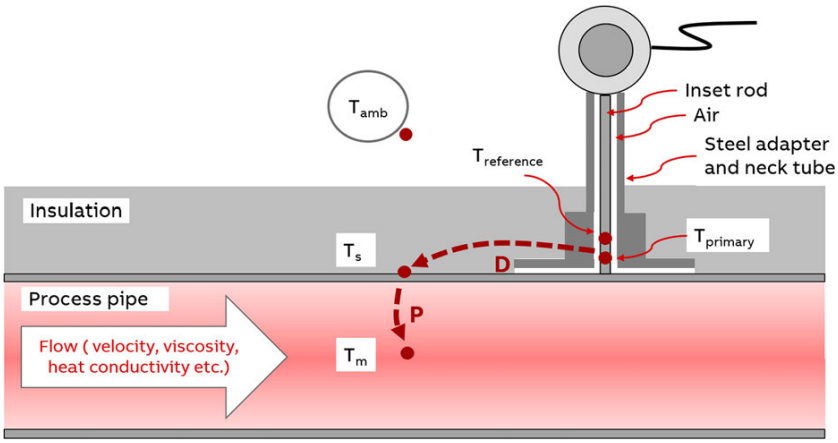

Figure 1: Two-Step-Approach: schematic of the approach to measuring the process temperature split into a process model (P) and a device model (D).

and implementation of temperature measurement while significantly enhancing the safety over traditional invasive approaches. The ability to infer the process temperature without the need for a penetration in the piping eliminates leak points, and minimizes the risks and costs associated with shutting down a running process to install a new measurement point. Critically, the temperature inference has to provide comparable, if not better, performance than traditional invasive approaches in terms of accuracy, repeatability and responsiveness to changes in the process temperature.

The current state of the art in temperature measurement that does not penetrate the piping are skin type or surface temperature sensors. Such sensors are widely used in the process industry and other contexts [3, 4, 5, 6]. However, they are considered to be less accurate and slower to respond than invasive measurements in a thermowell. In addition, the measurements can easily be influenced by ambient conditions such as convective currents, radiation or even outdoor effects [6]. The questions that need to be posed are whether their performance is a result of their construction and usage or if the inaccuracy and slower response are physically represented in the interaction of the pipe with the fluid.

In an industrial context, Gorman et al. [7] describe an approach to understand the measurement deviations of a surface measurement by considering the interaction of an uninsulated pipe carrying a process fluid with a surrounding ambient environment. Through dimensional analysis, a considerable number of parameters are organized to give an estimate that demonstrates a range of process conditions where a surface measurement is adequate. Nouri et al. [8] propose an elaborated shielded cable sensor setup for achieving reliable accuracy indicating clearly that the performance of the sensors can be improved with careful design.

However, what seems to be lacking is a validation of the application space for non-invasive measurements that considers both the static and dynamic requirements in industry.

In this paper we address this gap by first describing, in Section 2, a step wise model-based procedure for estimating the process temperature, with the surface temperature of the pipe as the primary physical measurement point.

In Section 3, analytical and CFD methods are developed to predict the temperature difference between a surface measurement on a pipe and the average bulk temperature of a flowing process medium. Organization of the use cases and the parameter sets for error estimates are done from an industrial end user's point of view. This means we aim at reducing the parameter space by imposing boundary conditions and parameters of relevant use cases. For the scope of this paper, we look primarily at important industrial cases where the analysis yields that the boundary layer resistance can be neglected.

Use case examples are considered in Section 4. Static and dynamic predictions of the models are tested first under controlled conditions on a test rig with water as the process medium. The performance of the models is then validated using results from real industrial applications of non-invasive sensors mounted in close proximity to traditional invasive ones.

2 Two-step measurement approach

The setup for a non-invasive temperature measurement in an industrial context is often similar to the one shown in Figure 1. A process medium is conveyed in a pipe that is protected against ambient conditions by one or several layers of insulating material. The outer surface of the insulation interacts with the ambient via convection and ra-

diation. The fluidś thermal interaction with the pipeś inner surface can often effectively be described by a thermal boundary layer with certain properties.

The situation is axisymmetric at this stage, and the thermal behavior of the setup in a steady state can be described by a linear chain of thermal resistances (see e. g. [5, 8] for previous work on this approach). Details of our specific formulation and use of the model are given in Section 3.1. We will call this the process model. If the parameters are known to sufficient accuracy, as well as two temperatures along the chain, an estimate of the medium temperature can be calculated. Among the challenges when using this model is knowing the thermal characteristics of the boundary layer.

The approach to determine an estimate of the medium temperature can therefore be divided into two steps. Having set up the process model, the next task is to accurately measure two temperatures, e. g. those of the pipe surface and the ambient.

In particular, finding a good estimate of the pipe surface temperature T_s is important and a challenge. Restricting ourselves to contact temperature sensors such as resistance temperature detectors or thermocouples, the sensor element, packaged for industrial environments, in some way has to be immersed in the insulation in order to make contact to the pipe surface. To some extent, the cylindrical symmetry characterizing the process model will be broken by conduction paths through the sensor in contact. Therefore, a specific type of model is needed to infer a good estimate of the surface temperature T_s, e. g., as indicated in Figure 1, from sensor readings $T_{primary}$ and $T_{reference}$. We will call this the device model. Details on the device model and the efficacy of devices using this approach can be found in previous publications (e. g. [9]) and will not be covered further. However, measurements using devices that incorporate this model will be shown and analyzed in later sections of this paper. The next section covers the development of analytical and numerical process models.

3 Process models, analytical and numerical

Models of the temperature measurement process can be used in different ways. First it is important to understand the physical situation of given use cases in order to determine applicability of a measurement concept. Some models can be embedded in intelligent devices (devices which have internal computation capabilities) for online measurement correction. Second, larger-scale offline simulations, e. g. involving CFD, can be used for benchmarking the embedded models. They are also relevant for understanding transient phenomena.

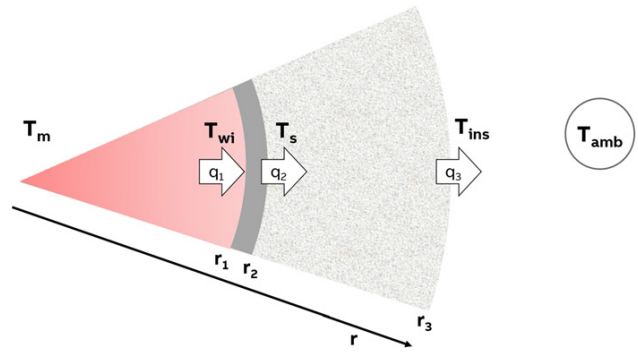

Figure 2: Schematic view of the axially symmetric temperature distribution. Notation and details are described in the text.

3.1 Analytical models and correlation formulae

Thermal interaction of fluid conveying pipes with their ambience has been extensively considered in literature (see, e. g., [10], and references therein). Assuming cylindrical symmetry one arrives at a one-dimensional description of the situation. It is shown schematically in Figure 2. In the figure, T_m is the fluid mean temperature, the target of the measurement process. T_m is generally defined via the convective heat flow $\dot{q}$ in the pipe, and the local flow of heat capacity $c_P \rho v$ is used as weight function when taking the mean over the pipe cross section A:

$$T_m := \frac{\int_A T c_P \rho v \, dA}{\int_A c_P \rho v \, dA}. \tag{1}$$

For a homogeneous flow ($\rho = const$ and $c_P = const$) the mean temperature is simply correlated to the flows of heat, mass and volume:

$$T_m := \frac{\dot{q}}{\dot{m} c_P} = \frac{\dot{q}}{\rho \dot{V} c_P}. \tag{2}$$

T_{wi} is the temperature at the inner wall surface. The temperature field is assumed to be continuous there. T_s is the temperature at the pipe surface. We assume that the contact resistance between insulation and pipe is negligible as compared to the insulation resistance. T_{ins} is the temperature at the outer surface of the insulation. T_{amb} denotes the ambient reservoir temperature in a certain distance from the isolation. q_i, $i = 1, 2, 3$ denote the heat flow densities at corresponding values of the radial variable r.

To describe the thermal layer resistances (which we define as temperature difference per heat flux), we start with the pipe flowś boundary layer. We use the definition of the Nußelt number

$$Nu_D := \frac{h_1 D}{\kappa_f} \tag{3}$$

where κ_f is the fluidś heat conductivity and h_1 is the hypothetical contact conductivity between fluid and inner wall surface (the conductivity of the fluid boundary layer). The pipe diameter D is taken as characteristic length scale. We then have for the heat flow density across the inner pipe surface

$$q_1 = Nu_D \frac{\kappa_f}{D}(T_m - T_{wi}) \ , \tag{4}$$

giving

$$R_{bl} = \frac{D}{Nu_D \, \kappa_f} \tag{5}$$

as the boundary layer resistance. For the temperature difference across the wall, the radial heat equation leads to

$$T_{wi} - T_s = q_1 \frac{r_1}{\kappa_w} \ln \frac{r_2}{r_1} = q_1 R_w \ , \tag{6}$$

with R_w as the layer resistance for the wall. The resistance of the insulation layer is, analogously,

$$R_{ins} = \frac{r_1}{\kappa_{ins}} \ln \frac{r_3}{r_2} \tag{7}$$

At the external surface of the insulation we generally may have convection with a coefficient h_3 and radiation

$$q_3 = q_1 \frac{r_1}{r_3} = h_3 \left(T_{ins} - T_{amb}\right) + \sigma\varepsilon \left(T_{ins}^4 - T_{amb}^4\right) \ , \tag{8}$$

where σ and ε are Stefan-Boltzmann constant and surface emissivity, respectively. The combined resistance R_{cr} of convection and radiation is

$$R_{cr} := \left[h_3 + \sigma\varepsilon \frac{(T_{ins}^4 - T_{amb}^4)}{T_{ins} - T_{amb}} \right]^{-1} \frac{r_1}{r_3} \tag{9}$$

In many cases, a detailed consideration of radiation can be avoided, since e. g. metallic low-emissivity covers can be used to ensure that radiative effects do not significantly contribute to heat transfer or can be included in an effective convection factor. Then we end up with just

$$R_{cr} := \frac{r_1}{h_3 r_3} \ . \tag{10}$$

The total resistance R_{tot} of the chain is given by

$$R_{tot} = R_{bl} + R_w + R_{ins} + R_{cr} \ . \tag{11}$$

From the definitions and the chain setup we arrive at the equation for calculation of T_m from measured quantities T_s and T_{amb} and known or estimated parameters:

$$T_m = T_s + (T_s - T_{amb}) \frac{R_{bl} + R_w}{R_{ins} + R_{cr}} \ . \tag{12}$$

As an example for a reasonable treatment of the boundary layer in turbulent flow range: For liquids as well as for gases, in this study we use the modified Petukhov-formula as proposed in [11, 12, 13, 14]

$$Nu_D^{turb} = \frac{(\xi/8) \cdot (Re - 1000) \cdot Pr}{1 + 12.7\sqrt{\xi/8}\left(Pr^{2/3} - 1\right)} \left[1 + \left(\frac{D}{L}\right)^{\frac{2}{3}} \right] \tag{13}$$

for

$$4000 < Re < 10^6 \text{ and } 0.1 < Pr < 10^3 \ .$$

The application range covers, e. g., large classes of water and gas flows. For the purpose of this work, effects of the entry length L are neglected. ξ should be calculated according to Konakov's formula [15]:

$$\xi = \xi(Re) = \frac{1}{(1.8 \cdot \log_{10} Re - 1.5)^2} \ . \tag{14}$$

This formula is valid in turbulent flows in approximately smooth pipes. For laminar flow ($Re < 2300$) the Nußelt number approaches $Nu_{D,lam} \approx 4$, the exact value depending on thermal boundary conditions. The transition region $2300 < Re < 4000$ can be covered by a linear interpolation.

For industrial purposes it is often of interest to consider the expected relative deviation $\Delta\theta$:

$$\Delta\theta := \frac{T_m - T_s}{T_m - T_{amb}} = \frac{R_{bl} + R_w}{R_{tot}} \tag{15}$$

It can now be estimated for a given use case, if medium, geometry and operation point for an industrial application are known. Certain parameters, e. g. regarding the insulation, can also be provided for the measurement points as a standard. In particular, regions can be determined where $\Delta\theta$ is small enough so that an online compensation for it is not necessary.

In a water application with a stainless steel pipe and mineral wool insulation of a prescribed thickness d_{ins}, for example, one may determine the range of allowed $\Delta\theta$ for a process run at approximately 60 °C as a function of pipe diameter D and flow velocity v. $\Delta\theta$ and the validity region with $\Delta\theta < 2\,\%$ are plotted in Figure 3.

These results are in good agreement with experiments and calculations given in Sections 4.2 and 4.3.

A full investigation of measurement uncertainties for the noninvasive measurement concept is beyond the scope of this paper. Nevertheless it makes sense to study the mea-

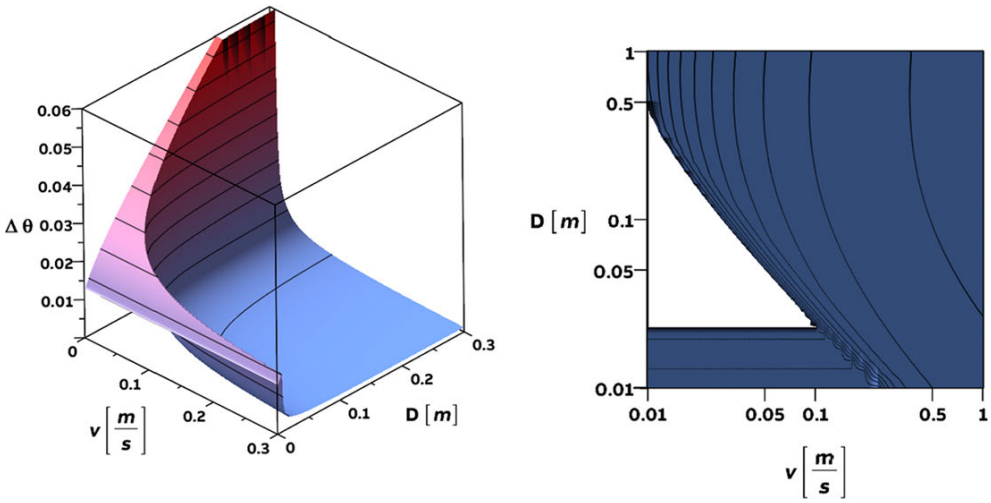

Figure 3: a) Estimate of relative deviation $\Delta\theta$ for a water process at approximately 60 °C as a function of pipe diameter D and flow velocity v (Parameters are: $\kappa_f = 0.67\,\mathrm{W\,m^{-1}\,K^{-1}}$; $\rho = 970\,\mathrm{kg\,m^{-3}}$; $\eta = 0.001\,\mathrm{Pa\,s}$; $Pr = 2$; $d_w := 2\,\mathrm{mm}$; $\kappa_w := 15\,\mathrm{W\,m^{-1}\,K^{-1}}$; $\kappa_{ins} = 0.045\,\mathrm{W\,m^{-1}\,K^{-1}}$; $d_{ins} = 0.1\,\mathrm{m}$; $h_3 = 4\,\mathrm{W\,m^{-2}\,K^{-1}}$). b) Region with $\Delta\theta < 2\,\%$ as a function of pipe internal diameter and flow velocity. (Note the double-log scale.)

Table 1: Measurement uncertainty assessment for an operation point with parameters as given in the text. The nomenclature mainly follows Ref. [16].

Input Variable	Unit	Value x	Relative Uncertainty u/x	Standard Uncertainty u	Sensitivity coefficient $\frac{dT_m}{dx}$	Induced standard uncertainty of T_m: $u \cdot \frac{dT_m}{dx}$ K	Induced variance of T_m: $\left(u \cdot \frac{dT_m}{dx}\right)^2$ K^2
T_s	°C	60	n/a	0.2	1.000E00	2.001E-01	4.003E-02
T_e	°C	20	n/a	0.5	3.469E-04	1.734E-04	3.008E-08
R_{bl}	$\frac{m^2K}{W}$	2.00E-04	0.25	5.00E-05	3.469E01	1.734E-03	3.008E-06
R_w	$\frac{m^2K}{W}$	2.00E-04	0.20	4.00E-05	3.469E01	1.387E-03	1.925E-06
R_{ins}	$\frac{m^2K}{W}$	1.08E00	0.10	1.08E-01	1.203E-02	1.303E-03	1.697E-06
R_{conv}	$\frac{m^2K}{W}$	7.04E-02	0.50	3.52E-02	1.203E-02	4.236E-04	1.794E-07
					Sum of variances: K^2		4.003E-02
Model result for T_m	°C	60.01			Combined standard uncertainty $u_c(T_m)$ K		2.001E-01

surement uncertainty associated to the model in Equ. 12 for an operation point which is representative for the experiments and use cases described in this article. Following [16], we perform a Type-B assessment with estimated uncorrelated uncertainties of the inputs in the model. As operation point we use the parameter set as given in Figure 3, now specifically for a DN80 pipe with a medium flow velocity of $v \approx 2\,\mathrm{m\,s^{-1}}$. This corresponds to a typical situation in the experiments described in Section 4.1. For simplicity and physical clarity, the uncertainty analysis is done on the level of temperatures and resistances. As inputs for the calculation, we assume standard uncertainties for the temperatures and relative uncertainties for the resistances. The calculation of the uncertainty $u_c(T_m)$ of the medium temperature measurement is given in Table 1.

We find that $u_c(T_m)$ is dominated here by the measurement uncertainty of the surface temperature T_s. It has been assumed to be 0.2 K. The model correction $T_m - T_s$ for the case is remarkably small, in the range of 10 mK. The situation is quite common for industrial processes with aqueous solutions as process medium, and for many others, too, such as steam applications. In particular, the analysis applies qualitatively to the experimental situations as described in Sections 4.1, 4.3 and 4.4.

3.2 Setup of CFD models

The correlation formulae used in the process model above are based on heuristics and experience from a large num-

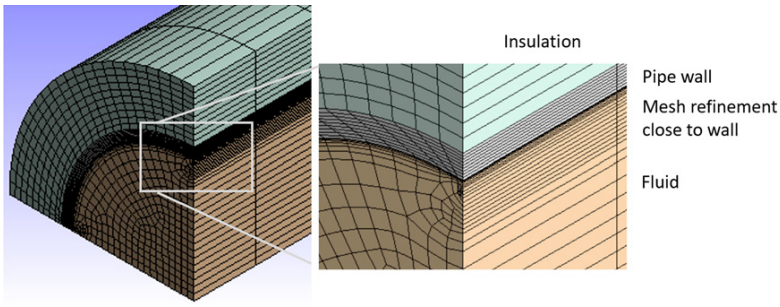

Figure 4: Illustration of the choice of the mesh for stable CFD-calculations. The inset shows the refined mesh in the vicinity of the pipe wall.

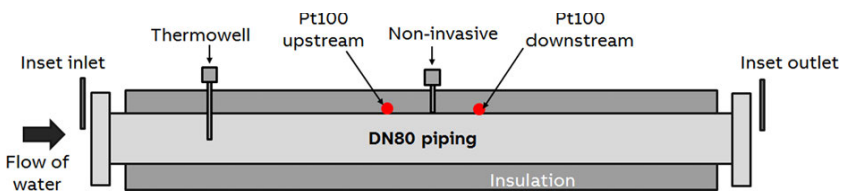

Figure 5: Schematic of the relative positioning of temperature sensors used in the experiments. The flow of the fluid is from left to right.

ber of measurements reported in literature. However, a drawback of these models is the inability to predict the thermal response of piping to changes in the temperature of the fluid. An well-known option is to do CFD calculations for studying conjugate heat transfer in pipes [17]. We use them here not only as a sanity check for the heuristic approach but also to understand transient phenomena.

The model solves equations of mass, momentum and energy conservation within the computational domain to calculate the flow and temperature fields. The k-ε-equations are additionally solved to resolve turbulent effects within the fluid. The flow was simulated to be hydrodynamically fully developed by imposing a power law velocity profile at the inlet. A mesh which was found to yield good convergence and stable results for this calculations is shown in Figure 4. Wall functions incorporated in the k-ε-formulation were imposed at the pipe wall, to resolve flow complexity there. In this way, the necessity of further near-wall mesh refinement can be avoided. The pipe model has a length of 4 m. Analyses of the radial temperature distributions have been done across a transverse section of the fluid and pipe, at the center of the 4 m pipe length. At the pipe outlet ambient pressure (gauge pressure equal to zero) was prescribed as the boundary condition. The velocity field within the pipe, as expected for turbulent flow, is almost uniform across the pipe, drastically reducing to zero at the wall.

In the next section, we compare and contrast some results from these inference models to measurements under test rig and real industry conditions.

4 Experimental results and industrial use cases

In this section, experiments from a test rig with water flow are described, and performance predictions for non-invasive measurements are analysed using the data. After that, we consider and evaluate test results for a water and a steam flow taken from measurement points in industrial plants.

4.1 Experimental setup: Turbulent flow of water in metal pipes

A set of experiments were carried out on a flow process test rig at ABB Corporate Research Germany. The flow rig consists of a system of tanks with the capability of pumping water through metal piping with standard flow rates ranging from 5 l/s to 20 l/s from one tank to another in a continuous closed loop system. The temperature of the fluid in the tanks is controlled by circulating a portion of the fluid contained in a tank through a heat exchanger system. Much like an industrial process facility, the rig is controlled by a distributed control system (ABB 800xA) and all sensor data are collected over a profibus DP system and stored in operational data historians. For the purposes of validating the performance of the process models, a comprehensive set of sensors were installed on a DN80 stainless steel pipe with a wall thickness of approximately 3 mm. The sensors are as follows (see Figure 5):

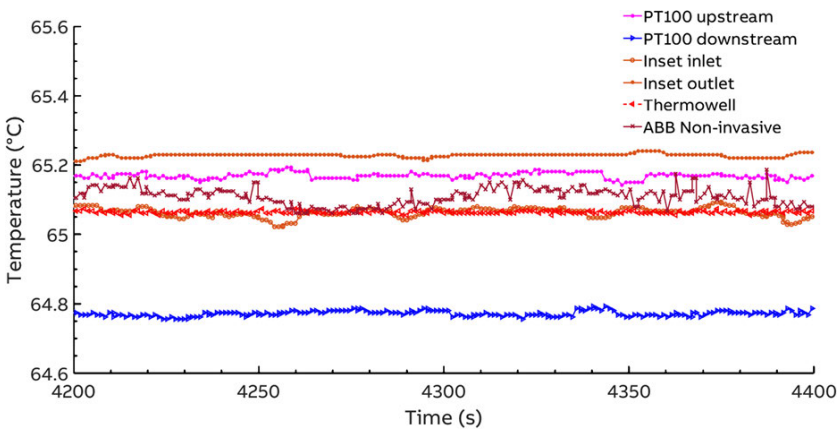

Figure 6: Subset of temperature measurements from all the sensors for the steady state flow of water through the flow rig. The set point temperature was 65 °C and held at that temperature for more than 70 minutes.

- Invasive measurement with standard 6 mm inset rods, without thermowell, approximately at the inlet and outlet of the straight measurement section,
- a standard 3G thermowell, mounted according to the state of the art, located 50 cm downstream of the start of the section,
- an ABB non-invasive temperature sensor with a device model located 1.5 m downstream of the thermowell,
- Pt100 sensors glued to the pipe surface below 5 cm of insulation, mounted approximately 50 cm upstream and downstream of the ABB non-invasive temperature sensor.

The experiments were started from ambient conditions in a climate controlled environment of 20 °C with the piping filled with water at close to the ambient temperature. The inlet and outlet valves were then closed and the water in the tank before the inlet heated to 65 °C. The pump was then started with the valve to the measurement section still closed until the set speed was achieved. The inlet valve was then opened with the pump pushing in hot water to replace the ambient temperature water in the piping such that the flow rises in an approximate stepwise manner. The valve opening time is in the range of 0.5 s to 1 s and the flow rate was approximately $\approx 10\,\mathrm{l\,s^{-1}}$, which corresponds to a flow velocity of $\approx 2\,\mathrm{m\,s^{-1}}$.

The response of all sensors was logged over the bus system with a logging frequency of 1 s. The experiments are carried out with a curtain separating the measurement setup from the rest of the room thereby creating an environment around the piping solely with natural convective currents. The experiments were run at a continuous process temperature of 65 °C for at least 1.5 h thereby ensuring that both the static and dynamic cases were adequately represented.

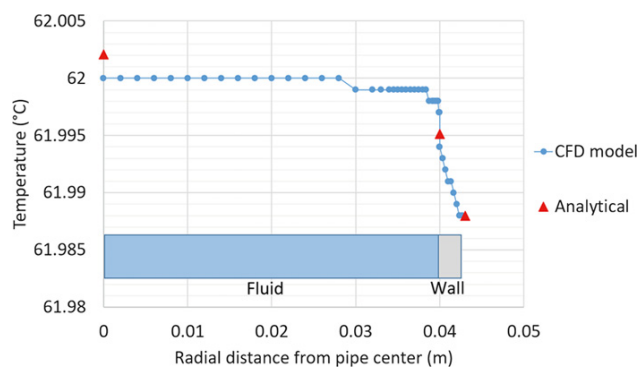

Figure 7: Comparison of predicted temperature profiles from CFD and analytical models for the experimental case of water flowing at $2\,\mathrm{m\,s^{-1}}$ in DN80 metal piping.

4.2 Comparison of models and experimental results

We start with the steady state response and then address the dynamic responses. Figure 6 shows the situation after complete thermalization of the rig. The maximum variation among all sets of measurements is less than ±0.5 °C. On this small scale, the deviation of one of the Pt100 sensors can be attributed to small differences in the glue-fixation to the pipe. Of particular interest is that the deviation between the measurement insets without the thermowell differs by less than 0.1 °C from the ABB non-invasive sensor and the Pt100s. This difference is generally insignificant in industrial applications. The close coincidence of surface measurements and fluid temperature is in line with predictions from the heuristic process model in Section 3.1 and CFD-calculations as outlined in Section 3.2. Model results are shown in Figure 7. Predicted differences between wall and water temperature are in the range of 0.01 °C. Both models start from the same pipe surface temperature. The analytical model estimate for the tempera-

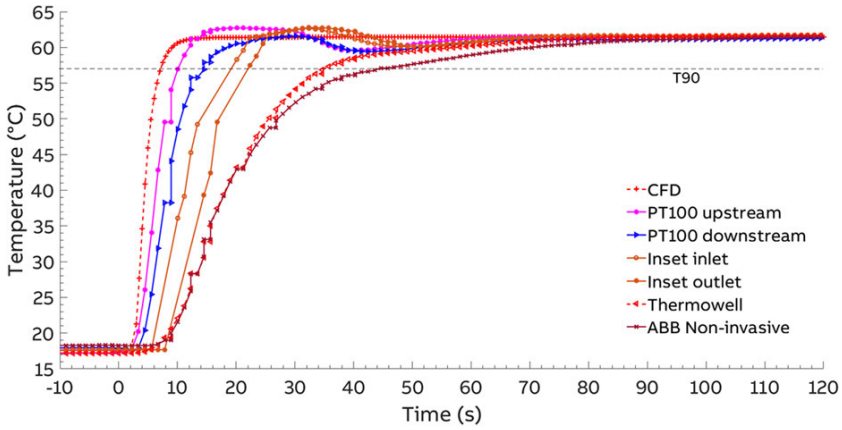

Figure 8: Dynamic response of temperature measurements with pumping hot water into the measurement pipe with a flow velocity of $2\,\mathrm{m\,s^{-1}}$. A temperature step from 17 °C to 62 °C is imposed and the T90 threshold is indicated.

ture difference to the process is ≈ 0.003 K larger than the CFD prediction.

We now examine the dynamic response. The results shown in Figure 8 demonstrate that the surface Pt100 measurements show the fastest response. The unshielded insets, surprisingly, are slower by about 5 s to 10 s. The response time T_{90} of the thermowell is ≈ 30 s to 35 s which agrees with specification for an optimally installed 3G thermowell. T_{90} for the non-invasive device is in the range of 35 s to 40 s with the device model designed to ensure no overshoot. The thermowell reaches standard accuracy of ±1 °C after about 35 s. The non-invasive device needs about 45 s, largely due to a remaining slow time constant in the setup. Both insets and the Pt100 register a slight ringing of the temperature signal which comes from the recirculation of room temperature water which was present downstream of the pump reentering the tank and cooling the incoming water slightly. This happens over a time scale that is faster than the response time of both the thermowell and the ABB non-invasive sensor.

Shown in the graph is also the predicted dynamic response of the CFD model showing a remarkably good match between rise time of the experimental measurements and that of the model. These results would indicate that CFD models could be used to predict the dynamic thermal response of non-invasive measurements for common process fluids.

In the next section, we present industrial use cases where the ABB non-invasive sensor is used as the reference of the surface response and is compared against invasive thermowells.

4.3 Industrial use case – Cooling water

Water and other cooling or heating fluids are widely used in heat exchangers in the process industry and naturally temperature is one of the critical parameters for control and monitoring purposes. For many of such use cases not all parameters for estimating the performance of a non-invasive measurement need to be known. By way of example, it suffices to know that a water-like is flowing and in a turbulent regime to know that a non-invasive temperature measurement is promising. A successful example has been investigated in long-term tests on a DN300 cooling water pipe. Based on the results in Figure 3 we expect good agreement with invasive measurements already for moderate flows. A snapshot of the results is given in Figure 9. Testing over several months, the average difference between the non-invasive and the thermowell measurement was 0.14 °C with a standard deviation of 0.13 °C. As demonstrated in this case, the non-invasive measurement meets the requirements of the application. A few data points show a large deviation from invasive measurements. They are connected to low-flow situations or even shutdowns where the thermal field starts to get highly inhomogeneous, and where both temperature measurements, therefore, are not representative.

4.4 Industrial use case – Steam measurements

Analytical correlation formulae and CFD calculations also suggest that there are certain classes of gas flows for which a non-invasive temperature measurement is promising. Due to its widespread and common use as a heating medium, we selected steam for a more detailed investigation. Here we present data from a district heating application where a non-invasive approach makes it easier to add distributed temperature measurements in the network without significant shutdowns.

In this use case, we consider a DN125 steam process pipe, insulated and conveying superheated steam at about

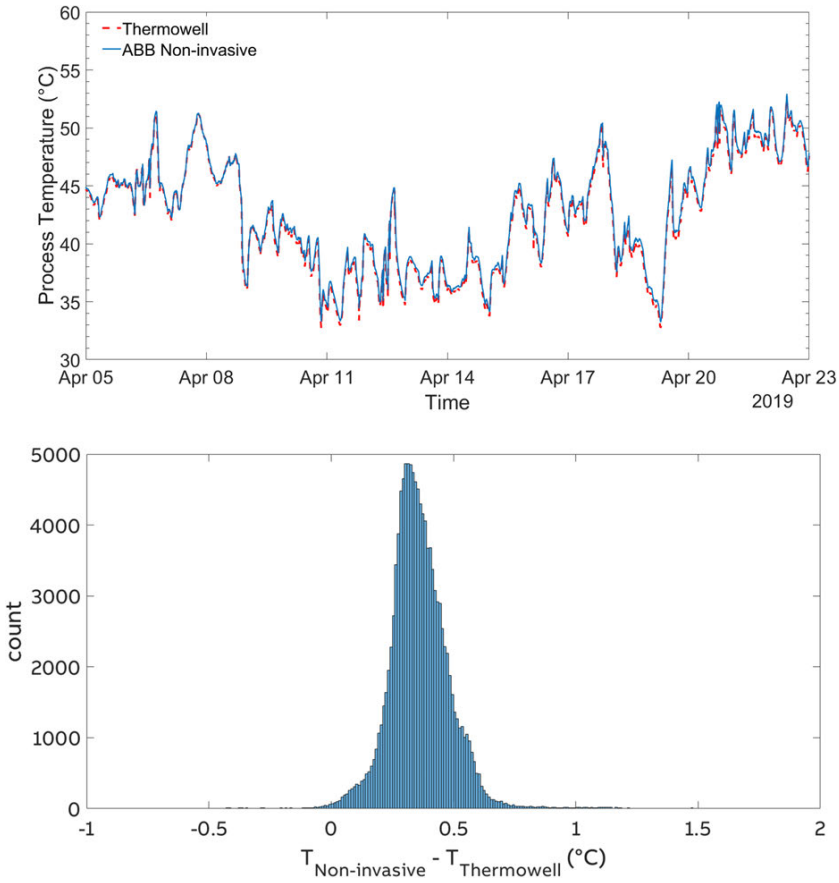

Figure 9: Process temperature measurements of cooling water from a non-invasive sensor mounted in the vicinity of a pre-existing thermowell. The upper figure shows a subset of the measurements over the course of several weeks. The lower figure shows the distribution of the difference between the non-invasive and thermowell measurements. The ambient temperature ranged from 5 °C to 15 °C.

Table 2: Temperature difference calculations by CFD and analytical formulae, for three flow values of superheated steam. All temperatures given in °C.

Flow condition		CFD model			Analytical result		
Flow rate	Re_D	pipe center	pipe outer wall	ΔT	pipe center	pipe outer wall	ΔT
1 t/h	1.53E+05	249.85	248.82	1.03	249.85	248.09	1.76
3.5 t/h	5.36E+05	249.96	249.39	0.57	249.96	249.26	0.70
5 t/h	7.65E+05	249.97	249.52	0.45	249.97	249.43	0.54

250 °C and approx. 10 bar and a flow rate between 1 t/h and 5 t/h. Table 2 shows that the predicted deviations differ, but are in the same acceptable order of magnitude. In particular, the total expected deviation is less than 1 % of the temperature difference between process and ambience.

Figure 10 shows an accuracy analysis of a corresponding benchmark test under industrial conditions. The non-invasive device is compared to an existing invasive temperature measurement which complies to the industry's standards. Although insulation was removed locally for this (indoor) test, the correspondence of thermowell and non-invasive measurement is remarkably good with an average of less than 0.1 °C difference between the two. The non-invasive device, interestingly, shows generally a slightly higher value than the invasive one. Among the reasons that could lead to this effect are heat conduction errors in the thermowell installation [3, 18], similar to those which have been studied in recent literature [19]. Of course, the remaining spread in the data can also be connected to the lack of a local insulation at the measurement point. The latter often is shielded quite well already by the stainless steel device adapter and small air gaps in the setup (shown in Figure 1). Nevertheless, if ambient effects are expected such as radiation, wind or generally time variations of the convective/radiative situation, a suitable insulation is recommended.

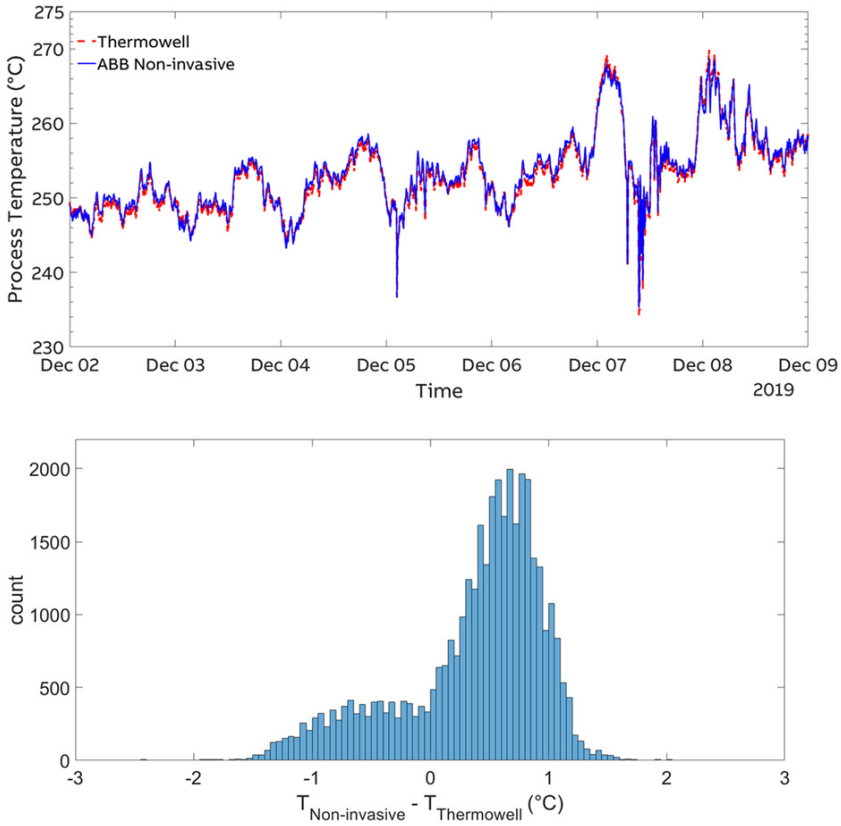

Figure 10: Process temperature measurements of steam from a non-invasive sensor mounted in the vicinity of a pre-existing thermowell. The upper figure shows a subset of the measurements over the course of several days. The lower figure shows the distribution of the difference between the non-invasive and the thermowell measurements. The pipe was located in a building.

5 Conclusions

A two-step approach to non-invasive temperature measurement on pipes has been proposed. It incorporates a process-pipe model based on well-known principles and heuristic thermo-hydrodynamic correlation formulae. The model is basically applicable in turbulent, transition and laminar ranges of process flow.

Two large classes of applications (with water and steam, respectively, as process media) have been addressed where process and pipe surface temperature can be estimated to be very close. Using CFD models, the analytical results could be cross-checked and predictions on transient behavior could be made for a temperature step in a water flow example.

In a corresponding test-rig experiment, responsiveness has been compared for a state-of-the-art industrial non-invasive device, a state-of-the-art thermowell, uncovered insets immersed in the water stream, and Pt100 sensors attached to the pipe surface. As predicted by CFD, the pipe surface temperatures react faster than even the uncovered insets. This shows the performance potential of surface measurements in this important type of application, which is obviously not limited by the physics of the boundary layer or pipe. The industry-compliant non-invasive device has been found in this test to be close in performance to the thermowell installations.

In a real-world cooling water application, long-term tests show that non-invasive and thermowell installation indeed deliver measurement results which are very close. A similarly good correspondence for a steam pipe measurement has been predicted analytically and by CFD. Subsequent measurements in an industrial steam use case confirmed the applicability of the concept.

Future work will include exploration of further use cases, according to their relevance, achievable accuracy and repeatability. Of particular interest for industry applications would be to investigate the robustness of measurement compensation in cases where R_{bl} can not be neglected, e. g. for gaseous processes at low flow and pressure.

References

1. U. Ahrend, M. Aleksy, M. Berning, J. Gebhardt, F. Mendoza, and D. Schulz. Challenges of the digital transformation: The role of sensors, sensor networks, IoT-devices, and 5G: Invited Paper. In *2019 First International Conference on Societal Automation (SA)*, Sep. 2019.

2. NAMUR – Interessengemeinschaft Automatisierungstechnik der Prozessindustrie e.V. Recommendation: Monitoring + Optimization (M+O)-Sensors. to be published, 2020.
3. ABB Measurement and Analytics. *Handbook of industrial temperature measurement: Basics and practice*. ABB Automation Products GmbH, 2013.
4. Thomas Köster. Temperaturmessung im regulierten Umfeld, Aktueller Stand der Technologien. *TechnoPharm*, 2(2):131–136, 2012.
5. F. Adunka. *Handbuch der Wärmeverbrauchsmessung*. Vulkan-Verlag, Essen, Germany, 5th edition, 2019.
6. Michael Pufke. Messtechnische Untersuchung von Rohranlegethermometern. PhD-Thesis, Technische Universität Ilmenau, Germany, 2019.
7. J.M. Gorman, E.M. Sparrow, and J.P. Abraham. Differences between measured pipe wall surface temperatures and internal fluid temperatures. *Case studies in Thermal Engineering*, 1, 2013.
8. B. Nouri, M. Röger, N. Janotte, and C. Hilgert. Characterization and corrections for clamp-on fluid temperature measurements in turbulent flows. *J. Thermal Sci. Eng. Appl.*, 10(3):13–16, 2018.
9. Jörg Gebhardt, Wilhelm Daake, Peter Ude, Karsten Schröder, and Guruprasad Sosale. Accurate and quickly responsive surface temperature measurement: a step to widespread non-invasive T-measurement in industry. In *IEEE International Instrumentation and Measurement Technology Conference*, I2MTC, Auckland, New Zealand, May 20–23, 2019.
10. Theodore L. Bergman, Adrienne S. Lavine, and Frank P. Incropera. *Fundamentals of Heat and Mass Transfer*. John Wiley & Sons, 7th edition, 2011.
11. J.P. Abraham, E.M. Sparrow, and W.J. Minkowycz. Internal-flow Nusselt numbers for the low-Reynolds-number end of the laminar-to-turbulent transition regime. *Int. J. Heat Mass Transfer*, 54:584–588, 2011.
12. V. Gnielinski. On heat transfer in tubes. *Int. J. Heat Mass Transfer*, 63:134–140, 2013.
13. V. Gnielinski. Corrigendum to “On heat transfer in tubes”. *Int. J. Heat Mass Transfer*, 81:638, 2015.
14. VDI-Gesellschaft Verfahrenstechnik und Chemieingenieurwesen, Karlsruhe, editor. *VDI-Wärmeatlas*. Springer, 12th edition, 2019.
15. Volker Gnielinski. Ein neues Berechnungsverfahren für die Wärmeübertragung im Übergangsbereich zwischen laminarer und turbulenter Strömung. *Forschung im Ingenieurwesen-Engineering Research*, 61(9):240–248, 1995.
16. Working Group 1 of the Joint Committee for Guides in Metrology. Evaluation of measurement data – Guide to the expression of uncertainty in measurement, JCGM 100:2008 (GUM 1995 with minor corrections). www.bipm.org/en/publications/guides/#gum (accessed 20th May 2020), September 2008.
17. B. John, S. Paramasivam, and S. Sadasivan. Applied and theoretical aspects of conjugate heat transfer analysis: a review. *Archives of Computational Methods in Engineering*, 26(12), January 2018.
18. F. Bernhard, editor. *Handbuch der technischen Temperaturmessung*. Springer-Verlag Berlin Heidelberg, 2014.
19. A. Brethauer, T. Fröhlich, and E. Engels. Comparison between different resistance thermometers at low immersion depths based on their heat conduction error. *tm-Technisches Messen*, 84(12):755–768, 2017.

Bionotes

Jörg Gebhardt
ABB Corporate Research Germany, Wallstadter Str. 59, 68526 Ladenburg, Germany
joerg.gebhardt@de.abb.com

Jörg Gebhardt is a Senior Principal Scientist at ABB Corporate Research in Ladenburg, Germany. He received his PhD in Theoretical Physics at University of Bonn in 1997. His research interests include physical modeling and simulation of sensor systems, development of new concepts for measurement instrumentation in industrial contexts, and new opportunities through digitalization.

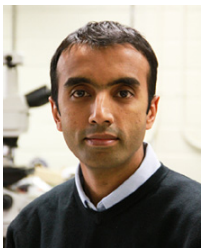

Guruprasad Sosale
ABB Automation Products GmbH, Industrial Automation – Measurement & Analytics, Kallstadter Strasse 1, 68309 Mannheim, Germany
guruprasad.sosale@de.abb.com

Guruprasad Sosale received his PhD in Mechanical Engineering in 2011 from McGill University in Montreal, Canada and worked as a senior scientist at ABB corporate research in Germany until November 2018. His research interests include design and development of novel sensing and communication concepts for the process industry. Based out of Mannheim Germany, he is currently the Global product manager for non-invasive and wireless technologies with ABB measurement and analytics.

Subhashish Dasgupta
ABB Global Industries and Services Pvt. Ltd, Bangalore, India
subhashish.dasgupta@in.abb.com

Subhashish Dasgupta, is a Ph. D. in mechanical engineering, from the University of Cincinnati, USA. His research topic was “Characterization of the thermal field generated by high intensity focused ultrasounds”. With his experience working as a post-doctoral research scholar in the Proctor and Gamble Simulation Center and subsequently research engineer in GE’s John F Welch Technology Center, in India, he joined ABB Corporate Research, India, in 2015. His research interest is primarily in multiphysics modeling, which includes computational fluid dynamics, heat transfer and electromagnetic analysis.